

Greenhouse gas emissions from laboratory-scale fires in wildland fuels depend on fire spread mode and phase of combustion

N.C. Surawski¹, A.L. Sullivan¹, C.P. Meyer², S.H. Roxburgh¹, and P.J. Polglase¹

¹CSIRO Land and Water Flagship and Agriculture Flagship, Clunies Ross St, Acton, ACT 2601, Australia

²CSIRO Oceans and Atmosphere Flagship, Station St, Aspendale, VIC 3195, Australia

Correspondence to: Nic Surawski (Nicholas.Surawski@csiro.au)

Abstract

Free-burning experimental fires were conducted in a wind tunnel to explore the role of ignition type and thus fire spread mode on the resulting emissions profile from combustion of fine (< 6 mm in diameter) Eucalyptus litter fuels. Fires were burnt spreading with the wind (heading fire), perpendicular to the wind (flanking fire) and against the wind (backing fire). Greenhouse gas compounds (i.e. CO₂, CH₄ and N₂O) and CO were quantified using off-axis integrated-cavity-output spectroscopy. Emissions factors calculated using a carbon mass balance technique (along with statistical testing) showed that most of the carbon was emitted as CO₂, with heading fires emitting 17% more CO₂ than flanking and 9.5% more CO₂ than backing fires, and about twice as much CO as flanking and backing fires. Heading fires had less than half as much carbon remaining in combustion residues. Statistically significant differences in CH₄ and N₂O emissions factors were not found with respect to fire spread mode. Emissions factors calculated per unit of dry fuel consumed showed that combustion phase (i.e. flaming or smouldering) had a statistically significant impact, with CO and N₂O emissions increasing during smouldering combustion and CO₂ emissions factors decreasing. Findings on the equivalence of different emissions factor reporting methods are discussed along with the impact of our results for emissions accounting. The primary implication of this study is that prescribed fire practices could be modified to mitigate greenhouse gas emissions from forests by judicious use of ignition methods to induce flanking and backing fires over heading fires.

1 Introduction

Wildfires emit a variety of pollutants to the atmosphere which have impacts on global warming, biogeochemical cycles, ambient air quality and human health (Mack et al., 2011; Monks et al., 2009; Weinhold, 2011). Globally, wildfires contribute approximately 23% of total anthropogenic greenhouse gas equivalent emissions (Houghton et al., 2009; van der Werf et al., 2010) although there can be significant year-to-year variability. Furthermore, increases in

wildfire occurrence have been observed in many parts of the world during the last decade, including the Western United States (Running, 2006), the Mediterranean region (Portugal, Spain and Greece) (Vicente et al., 2011) and Australia (Cai et al., 2009).

5 The main greenhouse gas species of interest emitted by wildfire include CO₂, CH₄ and N₂O. Wildfires also emit particulate matter (PM) to the atmosphere that has an impact on climate due to its ability to absorb and scatter light (Reid et al., 2005). In addition, the effect of wildfire PM on the aerosol indirect effect (i.e. cloud formation) remains poorly quantified at present (Bowman et al., 2009).

10 Despite considerable progress since the pioneering works on emissions from biomass burning by Crutzen et al. (1979), and Seiler and Crutzen (1980), only recently has the chemical composition of biomass burning smoke been quantified in detail. Yokelson et al. (2013) deployed a Fourier Transform Infra-Red Spectrometer (FTIR) and a range of different mass spectrometry systems to quantify 204 trace gas species, with a further 153 species being quantified but not able to be identified from the resulting mass spectra. Most of these
15 compounds were non-methane hydrocarbons which play a role in ozone and secondary organic aerosol formation (Akagi et al., 2011). Based on this work there now appears to be detailed knowledge on the chemical composition of smoke from biomass burning from fuels located in the south-east and south-west of the United States. Despite this new knowledge, measurements of N₂O emissions from biomass burning are not commonly reported
20 (Meyer and Cook, 2015, In press).

The various sections of free-burning wildland fire perimeters propagate with three distinct orientations in response to the prevailing wind direction. Fire perimeters can propagate with the wind (i.e. a heading fire) against the wind (i.e. a backing fire) and perpendicular to the wind (i.e. a flanking fire) (Sullivan et al., 2012). The individual fire spread modes (i.e. heading, flanking and backing) within a larger overall fire exhibit different fire behavior (such
25 as different rates of spread, flame heights, combustion factors and fireline intensities) which could lead to differences in emissions with respect to fire spread mode (Sullivan and Ball, 2012).

Laboratory experiments testing the role of fire spread mode on fire behavior and emissions have been conducted previously with Keene et al. (2006) referring to flanking fires as mixed combustion fires. Keene et al. reported differences in modified combustion efficiency (MCE) with different fire spread modes and report higher emissions factors for acetic acid (CH_3COOH) for heading and flanking fires compared to backing fires. However, the only greenhouse gas compound measured in the study of Keene et al. was CO_2 , although, detailed particulate emissions measurements were made.

In this study, we re-examine the burning methodology of Keene et al. in a controlled laboratory study involving a free-moving fire. We developed an explicit experimental design combined with statistical testing of results to examine the hypothesis that greenhouse gas emissions could depend on fire spread mode. The validity of this hypothesis has the implication that if emissions were dependent on fire spread mode, opportunities could open up to dramatically improve the precision with which greenhouse gas estimates of wildfire events are made and, perhaps more importantly, to strategically manage prescribed burning operations in forested landscapes to minimise greenhouse gas emissions by changing the applied fire spread mode of such fires.

In this study, the impact of fire spread mode on greenhouse gas (CO_2 , CH_4 , N_2O) emissions (plus CO) profiles from the combustion of dry eucalypt forest litter was tested in a combustion wind tunnel facility. Dry eucalypt forest fuel was selected for this study as it is the dominant flora of south-eastern Australia with this region being representative of fire activity in Australian temperate forests. Emissions estimates derived from this study build upon previous research efforts undertaken globally in temperate forest, where it is noted that emissions estimates from this ecological biome are rare in Australia (van Leeuwen and van der Werf, 2011).

In addition to testing the role of fire spread mode (i.e. heading, flanking and backing) on greenhouse gas emissions, the role of combustion phase (i.e. flaming or smouldering) and the temporal progression of emissions factors during a complete fire are explicitly tested with appropriate statistical methods. We also report findings on different methods for reporting emission factors and demonstrate the impact of our results with reference to green-

house gas emissions accounting from prescribed burning in Australia. Overall, the results from this study provide a new body of information on biomass burning emission estimates from a region that has been poorly characterised in the past.

2 Methodology

2.1 Combustion wind tunnel details

Experiments were conducted in the CSIRO Pyrotron (see Fig. 1) which is a 25.6 m long combustion wind tunnel facility designed to investigate the behaviour and emissions of laboratory-scale fires (Sullivan et al., 2013). Wind for experiments is generated upstream from the working section by a 1.372 m diameter centrifugal fan (model 54LSW) from Fans and Blowers Australia Pty Ltd. Positioned downstream of the fan in the settling section are four perforated screens and a flow straightener for removing as much turbulence from the air stream as possible (turbulence intensity < 0.6%) (Sullivan et al., 2013). The working section, where fuel is placed for experimental burns and where combustion takes place, is 1.5 m wide and 4.8 m long. Gas phase emissions samples were obtained from the exit section of the wind tunnel, downstream of the working section. Two 12.7 mm diameter stainless steel tubes positioned at a height of 840 mm above the floor of the combustion wind tunnel were used to sample gas and particle phase samples separately. An array of K type thermocouples are positioned on the floor of the CSIRO Pyrotron with a spacing of 500 mm in the direction of wind flow with a least 11 thermocouples spanning the width of the working section to record temperatures at the flame base (Sullivan et al., 2013). The design of the CSIRO Pyrotron enables sampling from the plume of a low intensity free-moving fire, driven by the wind, which may be contrasted with the approaches used by, for example, Lobert et al. (1990), McMeeking et al. (2009) and Jenkins et al. (1993) which all involve stack sampling without capturing either the free-moving or wind-driven characteristics of wildland fires.

2.2 Fuel collection and preparation

Forest litter fuel was collected from Kowen Forest in the north-east of the Australian Capital Territory (ACT), Australia during late summer (see Fig. 2), in a stand dominated by *Eucalyptus macrorhyncha* (F. Muell.) and *E. rossii* (R.T. Bak. & H.G. Sm.). The fine fuel (< 6 mm diameter) litter layer was collected because it is the primary fuel layer combusted during forest fires in south-eastern Australia (Sullivan et al., 2012) and was comprised of leaf, bark and twig components. An attempt was made during the fuel collection not to include coarse fuel elements (such as large pieces of bark, twigs, logs and branches) greater than 6 mm in diameter. Fuel was sieved after collection to remove coarse fuel fractions that were not removed in the field. Fuel sieving also removed fragmented material from the soil fermentation layer which can affect the ability of a fire to propagate and its combustion phase.

A dry fine fuel load of 1.1 kg m^{-2} (or 11 t ha^{-1}) was used which is typical of dry sclerophyll forest and is equivalent to that experienced during a major Australian wildfire (the 2009 Kilmore East fire) in dry sclerophyll forest (with a low understorey) in Victoria (Cruz et al., 2012)). The moisture content of the fuel was measured prior to weighing to ensure that the correct dry fuel weight was achieved. Fuel moisture measurements before fuel drying were performed with a Wiltronics fine fuel moisture meter (Chatto and Tolhurst, 1997) which uses the electrical resistance of a plant sample to measure its water content.

After weighing out the fuel with ambient moisture content it was dried in an oven at 50°C for 24 hours to reduce the fuel moisture content to a level typical of that for fine fuels during major Australian wildfires (< 5% oven-dry weight) (Cruz et al., 2012; McArthur, 1967; Sullivan and Matthews, 2013). Prior to each experimental burn, three to five sub-samples were collected in tins from the fuel bed to measure the fuel moisture content. The tins were oven-dried at 105°C for 24 hours (Matthews, 2010) with fuel moisture contents between 4.6–6.8% being achieved (see Table 1).

Fuel was spread in the working section of the wind tunnel to make the fuel bed as homogeneous as possible in terms of depth and the structural arrangement of leaf, bark and twig components. Mean fuel depths were between 24.2 and 33.6 mm for the experimental fires.

Three unburnt fuel samples were sorted and weighed throughout the course of the experiment to establish the relative proportions of leaf (23.2%), bark (28.6%) and twig (48.2%) components. The size of the fuel bed was 6 m² (4 m × 1.5 m) for heading fires and 2.25 m² (1.5 m × 1.5 m) for flanking and backing fires.

5 Fires were ignited using a 1.5 m channel filled with ethanol (60 ml volume), which was placed in a different position (relative to the air flow) for each fire spread mode and lit with a gas lighter. Each fire spread mode was replicated six times (with the level of replication being based on Mulvaney (2012) to enable the experimental uncertainty to be reduced to a satisfactory level. This level of replication resulted in a total of 18 fires. A wind speed of 1.5
10 m s⁻¹ was used in all fire experiments. Altogether, the selection of fuel loads, fuel moisture content and wind speed were selected to achieve Byram fireline intensities (Byram, 1959) (which is the product of the lower heating value of the fuel, fuel consumed and the forward rate of spread) indicative of those during prescribed burning conditions in temperate eucalypt forest in Australia (i.e. approximately < 500 kW m⁻¹ (Cheney, 1981) or approximately
15 < 345 kW m⁻¹ (McArthur, 1962)).

2.3 Emissions measurements

Gas phase measurements were performed using off-axis integrated-cavity-output spectroscopy (off-axis ICOS), a laser-based absorption technique used in commercially available instruments from Los Gatos Research (<http://www.lgrinc.com/>). One instrument measured CO₂/CH₄ (Greenhouse Gas Analyser GGA-24r-EP) and the other measured N₂O/CO (N₂O/CO Analyser 907-0015) with both instruments operating in slow flow mode. The method works by directing a laser beam into an optical cavity equipped with high reflectivity dielectric coated mirrors (with mirror losses around 100 ppm capable of being achieved) (Baer et al., 2002). The absorption signal is determined by the temporal decay (or 'ring-down') of the light transmitted through the cavity due to absorption (based on the Beer-Lambert law) which is modelled as an exponential decay process (O'Keefe and Deacon, 1988).
20
25

Due to the highly reflective nature of the mirrors, optical path lengths of several kilometres can be achieved, making the technique highly suited for the detection of trace gas species (Baer et al., 2002). Off-axis ICOS is a relatively new method in cavity ring down spectroscopy that is simpler to operate as the optical alignment of the laser beam with respect to the optical cavity does not need to be mode-matched (Baer et al., 2002). Both instruments collected data with a 1 Hz sampling frequency. Particle phase emissions measurements were also made during experiments, but we reserve the presentation of those results for a future publication.

For gas measurements, the sample flow was diluted with zero air (i.e. 20.5% O₂ in N₂) to enable simultaneous quantification of N₂O and CO. During calibrations (Fig. 3) there was spectral broadening of the CO absorbance peak with smouldering combustion (CO concentrations in excess of 10 ppm) which prevented the N₂O absorbance peak from being quantified accurately. To keep the CO concentration below 10 ppm and prevent the spectral broadening, a dilution ratio between 5.7 and 6.0 for flanking and backing fires and between 5.9 and 10.7 for heading fires were used. Heading fires required the initial dilution ratio to be increased during the experiment which is why these dilution ratios are greater than those for flanking and backing fires.

Calibration of the N₂O/CO instrument (before and after experiments) against bottled CO gas gave coefficients of determination of 0.9993 and 0.9996 based on a linear fit between the measured CO concentration and the concentration provided by the calibration system, with slopes of these linear fits being 0.94 and 1.07. Overall, the calibrations performed before and after experiments confirmed the linear response and accuracy of the off-axis ICOS technique.

2.4 Data analysis

2.4.1 Calculation of emissions factors

Emissions ratios are widely used in biomass burning research to rectify the problems associated with plume sampling in environments subject to variable levels of dilution (Le Canut et al.,

1996) and as such are used as an input to enable the calculation of emission factors. An emissions ratio (ER) is calculated via the following equation (Levine and Cofer III, 2000):

$$ER = \frac{\Delta X}{\Delta \text{Reference Gas}}, \quad (1)$$

where X is the gas of interest, the reference gas is usually either CO or CO₂ (although CH₄ is sometimes used), and Δ is the excess mixing ratio which denotes that the smoke-free ambient concentration is subtracted from the plume concentration (i.e. $\Delta X = X_{plume} - X_{ambient}$).

The selection of the reference gas is based on the quality of a linear fit between excess mixing ratios of the gas of interest (Y axis) and the reference gas (X axis). The slope of the resulting linear fit therefore provides another method for quantifying an emissions ratio. Figure 4 shows correlation plots for incomplete combustion products using either CO₂, CO, or CH₄ as a reference gas. The best linear fit was obtained for CH₄ using CO as a reference gas ($R^2=0.942$) and by using CH₄ as a reference gas for N₂O emissions ($R^2=0.822$). Overall, the degree of fit with all three reference gases was similar, so CO₂ was used as a reference gas since it is the dominant carbon-containing compound in the plume and it is also a relatively simple gas to measure (Levine and Cofer III, 2000).

A carbon mass balance approach developed by Radke et al. (1988), and applied (for example) by Lobert et al. (1990), Hurst et al. (1994a), Hurst et al. (1994b) and more recently by Meyer et al. (2012), was used to calculate emissions factors for different carbon- and nitrogen-based pollutants on a per unit element burnt basis. Calculating emissions factors this way enables the fraction of carbon (or nitrogen) emitted from different chemical compounds containing that element to be quantified. Using CO₂ as a reference gas for all carbon containing species, the emissions factor for carbon dioxide (EF_{CO_2}) is given by:

$$EF_{CO_2} = \frac{\sum C_{emit}}{C_{fuel}} \frac{1}{1 + \frac{\Delta CO}{\Delta CO_2} + \frac{\Delta CH_4}{\Delta CO_2} + \frac{\Delta \sum NMHC}{\Delta CO_2} + \frac{\Delta PC}{\Delta CO_2}}, \quad (2)$$

where C_{emit} is the mass of carbon emitted to the atmosphere, C_{fuel} is the mass of fuel carbon burnt, NMHC represents the sum of all non-methane hydrocarbons, and PC repre-

sents particulate carbon. NMHC have not been quantified in the current study; however, to complete the calculation of emissions factors in the above equation, an NMHC emissions factor of 0.0091 has been used based on the fire emissions work of Hurst et al. (1994a) in Australian savanna's. Note that there are no published estimates of PC emissions factors in Australian temperate forest so this term has been removed from the calculation of emissions factors. Removing PC emissions factors from the calculation of emission factors would have a very marginal impact on the final results with an upwards bias of < 1–2% being likely (Yokelson et al., 1999).

To calculate carbon-based emission factors for compounds other than CO₂ the following equation was used:

$$EF_X = \frac{\Delta X}{\Delta CO_2} n EF_{CO_2}, \quad (3)$$

where n is the number of carbon atoms in the compound of interest.

By definition, the sum of all carbon-based emission factors equals the fraction of fuel carbon that is emitted to the atmosphere. This expression is given by:

$$\sum_X EF_X = \frac{\sum C_{emit}}{C_{fuel}}. \quad (4)$$

To estimate emissions factors for N₂O, the excess mixing ratio for N₂O is substituted into the numerator of equation (3) and is then divided by the molar nitrogen-to-carbon ratio of the fuel to account for the fact that every mole of N₂O has two moles of N. Performing this calculation makes nitrogen-based emission factors independent of the nitrogen content of the fuel (Hurst et al., 1994b). Nitrogen-to-carbon ratios (0.73%) were measured from unburnt fuel samples, consisting of leaf, bark and twig components, using Isotope Ratio Mass Spectrometry.

Whilst reporting emissions factors on a per unit element basis is common in inventory reporting, in atmospheric chemistry it is common to report emissions factors per unit of dry fuel consumed. The carbon mass balance method used to present emissions factors this

- 5 way is discussed by Yokelson et al. (1999) and Paton-Walsh et al. (2014) and for carbon containing species is given by the following equation:

$$EF_i = F_c \times 1000 \times \frac{MM_i}{12} \times \frac{C_i}{C_T}, \quad (5)$$

- where EF_i is the mass of compound i emitted per kg of dry fuel consumed, F_C is the fractional fuel carbon content (measured before burning: 0.516), 1000 is a units conversion factor (1000 g kg⁻¹), MM_i is the molecular mass of species i , 12 is the atomic mass of carbon, C_i/C_T is the number of moles of species i emitted divided by the total number of moles of carbon emitted.

When using CO₂ as a reference gas, C_i/C_T is given by:

$$\frac{C_i}{C_T} = \frac{\frac{\Delta C_i}{\Delta CO_2}}{\sum_j NC_j \frac{\Delta C_j}{\Delta CO_2}}, \quad (6)$$

- 15 where ΔC_i and ΔC_j are the excess mixing ratios for species i and j and NC_j is the number of carbon atoms in species j .

To calculate N₂O emissions factors per unit of dry fuel consumed, the following equation (based on Andreae and Merlet (2001)) was used:

$$EF_{N_2O} = ER_{N_2O/CO_2} \times \frac{MM_{N_2O}}{MM_{CO_2}} \times EF_{CO_2}. \quad (7)$$

- 20 This equation uses a molar emissions ratio for N₂O/CO₂, the CO₂ emissions factor and the respective molecular masses to calculate an emissions factor.

2.4.2 Other calculations

Time series data of excess mixing ratios was calculated by subtracting the diluted ambient readings for emissions before the test from the plume diluted concentrations, as the emissions from the fire only (and not ambient air) were of interest. Concentrations were then multiplied by the dilution ratio to enable undiluted plume concentrations to be calculated.

Emissions factors reported on a per unit dry fuel consumed basis were estimated (using equation (5) for carbon containing species and equation (7) for N_2O) separately for the flaming and smouldering combustion phases of each fire. Furthermore, plotting the results of equations (5) and (7) versus time enabled time series of emissions factors ($g\ kg^{-1}$) to be calculated.

2.4.3 Statistical analysis of data

Multivariate Analysis of Covariance (MANCOVA) was performed to test for the statistical significance of fire spread mode (a categorical factor) and fine fuel moisture content (a numerical covariate) on the emissions factors measured. The one-way MANCOVA analysis involved testing hypotheses related to a single categorical variable and a single numerical covariate. The statistical models fitted to the data were of the following form:

$$Y_{ijk} = \underbrace{\mu}_{\text{Grand mean}} + \underbrace{\alpha_{ij}}_{\text{Treatment effect}} + \underbrace{\beta_{ij}}_{\text{Covariate effect}} + \underbrace{\epsilon_{ijk}}_{\text{Residual}} \quad (8)$$

where Y_{ijk} is the response (i.e. the emissions factor) for the i th emissions species for the j th fire spread mode and for the k th replicate.

The null hypothesis (H_0) being tested for the categorical variable (fire spread mode) was:

$$H_0 : \mu_{iH} = \mu_{iF} = \mu_{iB} \text{ for } \forall i, \quad (9)$$

where H , F and B denote the levels of the fire spread mode factor (i.e. heading, flanking and backing fires).

This hypothesis states that different fire spread modes (i.e. heading, backing and flanking) do not lead to significant differences in emissions for all species investigated (i.e. CO_2 , CO , CH_4 , N_2O and residue carbon).

The alternative hypothesis (H_1) being tested was that at least one of the μ_{ij} comparisons in equation (9) were concluded to differ.

The null hypothesis being tested for the covariate (fine fuel moisture content) was:

$$H_0 : \beta_{iH} = \beta_{iF} = \beta_{iB} \text{ for } \forall i, \quad (10)$$

while the alternative hypothesis tested that at least one of the β_{ij} slope comparisons in equation (10) were concluded to differ.

In addition, Multivariate Analysis of Variance (MANOVA) was performed to test whether fire spread mode and combustion phase (i.e. flaming or smouldering combustion) had a statistically significant impact on emissions factors reported on a per unit dry fuel consumed basis. The statistical models fitted and hypotheses tested had the same structure as equation (8), except instead of having a single factor and a covariate, two categorical factors (i.e. fire spread mode and combustion phase) were fitted in this two-way MANOVA. All statistical tests were conducted using R v 3.03 and a significance level of 5% was used to determine statistical significance.

3 Results

Table 1 reports summary statistics from the fire experiments which shows that flanking and backing fires are quite similar in terms of their Byram fireline intensity (Byram, 1959), rate of spread and duration of smouldering combustion. Heading fires burnt about 20 times faster (for rate of forward spread) and with approximately 20 times higher fireline intensity than flanking or backing fires. Furthermore, the duration of flaming combustion was about 75% less with heading fires and smouldering combustion was more than twice as long. Table 2 reports emissions factors for all four emissions species per unit dry fuel consumed.

Time series data for the excess mixing ratios of CO_2 , CO , CH_4 , and N_2O are shown in Fig. 5. The two most striking aspects are the relative magnitudes of the emissions peaks, and also differences in the combustion duration for different fire spread modes. Heading fires produced very pronounced peaks during flaming combustion for all emissions species considered, whereas flanking and backing fires exhibit less temporal variability in their emis-

5 sions with less pronounced peaks. The temporal variability in emissions is very similar for flanking and backing fires.

Emissions factors for carbon- and nitrogen-based species using the carbon mass balance approach show that between 63–74% of fuel carbon is emitted to the atmosphere as CO₂, and about 5.7–13% is emitted as CO (Fig. 6), 0.36–0.53% as CH₄ and 0.35–0.57% of fuel
10 nitrogen as N₂O (Fig. 6). For heading fires, the CO₂ emissions factor was about 17% greater than flanking fires and 9.5% higher than backing fires and CO emission factors were about twice as high for heading fires than for the other two fire spread modes. The fraction of unburnt and partially burnt fuel (residue) ranges from 12% of fuel carbon for heading fires
15 up to 30% of fuel carbon for flanking fires. During some experiments, it was difficult to get flanking fires to propagate with a continuous flame front which offers an explanation for the greater production of combustion residue (due to patchiness) during these fires.

Statistical testing of the results with MANCOVA indicated that fine fuel moisture content (i.e. the covariate) did not have an impact on emissions factors ($p = 0.60$); however, fire spread mode was a statistically significant factor ($p < 0.0001$). Fire spread mode had a
20 statistically significant effect on CO₂ ($p < 0.0001$), CO ($p < 0.0001$) and carbon residue production ($p < 0.0001$) but did not have a statistically significant effect on CH₄ ($p = 0.269$) or N₂O emissions ($p = 0.261$). Testing with pairwise comparisons showed that CO₂ emissions factors for all paired combinations of fire spread mode (i.e. heading versus backing, heading versus flanking and flanking versus backing) were statistically different ($p < 0.0001$
25 for all comparisons). For CO emissions, heading versus backing and heading versus flanking emissions factors were statistically different ($p < 0.0001$ for all comparisons); however, flanking emissions factors were not statistically different to backing emissions factors ($p = 0.962$).

As shown previously (see Fig. 6), emissions factors for different chemical species varied significantly with respect to fire spread mode. In addition, the different phases of combustion (e.g. flaming, smouldering, and glowing) during a fire have different fire behaviour and, therefore, potentially different emissions profiles (Lee et al., 2010). To test this hypothesis, emissions factors (per unit of dry fuel consumed) were calculated separately for flaming and

5 smouldering phases for the 18 experimental fires (see Fig. 7). In this paragraph we discuss the numerical trends found, whilst the next paragraph discusses testing of our results for statistical significance. Numerically, the results confirm that both CO and CH₄ emissions factors were substantially increased during smouldering combustion. CO emissions factors ranged from 72–102 g kg⁻¹ during flaming combustion and ranged from 189–221 g kg⁻¹ during smouldering combustion. CH₄ emissions factors ranged from 2.4–3.8 g kg⁻¹ during flaming combustion and 5.0–10.5 g kg⁻¹ during smouldering combustion. With more carbon being emitted as either CO or CH₄ during smouldering combustion, this led to decreases in the CO₂ emissions factor, with CO₂ emissions factors ranging from 1705–1750 g kg⁻¹ during flaming combustion and from 1515–1550 g kg⁻¹ during smouldering combustion. Numerically, N₂O emissions factors did not increase during smouldering combustion for heading fires but did increase for both backing and flanking fires.

The MANOVA analysis confirms that combustion phase ($p < 0.0001$) had a statistically significant impact on emissions factors (reported per unit of dry fuel consumed) and so did fire spread mode, but only for the heading fire versus flanking fire comparison ($p = 0.04$). CO₂ emissions factors were lower during smouldering combustion ($p < 0.0001$) whilst CO emissions factors were increased ($p < 0.0001$). CH₄ emissions factors did not exhibit statistically significant differences with respect to combustion phase ($p = 0.12$) but N₂O emissions factors did ($p = 0.04$). Whilst the non-significant result for CH₄ may appear to contradict the trends discussed in the previous paragraph, the CH₄ results are more variable which prevents a statistically significant result from being found. Furthermore, N₂O emissions factors exhibited a relationship with fire spread mode ($p = 6.5 \times 10^{-3}$) with heading fires producing less N₂O than flanking or backing fires.

Time resolved emissions factors (on a per dry fuel consumed basis) were calculated and are shown in Fig. 8. This graph shows that the CO₂ emissions factor peaks early in the burn during flaming combustion with a pronounced decrease (with an increase in CO) after the passage of the flame front through the fuel bed. CH₄ and CO emissions factors are quite low during flaming combustion, but increase significantly once smouldering combustion starts to

dominate. N_2O emissions show a significant contribution from both flaming and smouldering combustion.

4 Discussion

4.1 Representativeness of combustion wind tunnel emissions measurements

Since emissions sampling was conducted at a single fixed height above the wind tunnel floor (see section 2.1), further analysis needs to be conducted to ensure the representativeness of measurements. If chemical reactions were still occurring at the axial position of sampling, and if those reactions had a dependence on sampling height, then the emissions measurements obtained would not be representative of the entire plume. Here we calculate the reaction Damköhler number (Da) (Law, 2006, p. 189) which characterises the ratio of the flow time scale (τ_F) to the chemical reaction time scale (τ_C). The reaction Damköhler number is given by:

$$\begin{aligned}
 Da &= \frac{\text{Characteristic flow time}}{\text{Characteristic reaction time}} \\
 &= \frac{\tau_F}{\tau_C} \\
 &= \frac{kL}{\bar{U}}
 \end{aligned} \tag{11}$$

where τ_F is given by the characteristic length scale (L) divided by the characteristic velocity (\bar{U}) (Law, 2006) and τ_C is the reciprocal of the reaction rate (k). We choose L as the axial distance from the flame position to the sampling manifold (either 3.6 or 8.4 m), \bar{U} as the mean wind speed employed during testing (1.5 m s^{-1}) with k given by the lumped kinetic scheme of Ranzi et al. (2008), which describes the production of CO_2 , CH_4 and CO (plus other carbon compounds) from biomass pyrolysis. We calculate k at two heights within the flame, with maximum temperatures at the flame base being based on those recorded by thermocouples on the CSIRO Pyrotron floor, whilst flame tip temperatures are based on

measurements made in eucalypt shrubs by Wotton et al. (2012). Calculation of the reaction Damköhler number enables us to assess how close the relevant chemical reactions are to equilibrium at two flame heights and axial positions within the flow, with the results of this calculation being shown in Table 3.

We see that the reaction Damköhler number depends on vertical position within the flame, with smaller Da being observed at the flame tip (i.e. 3.0×10^6) compared to the flame base (1.8×10^8 – 2.9×10^8). There is also variation in the Da observed with different fire spread modes which is due to differences in the maximum flame base temperature and the influence it has on reaction kinetics. Whilst we see variation in Da with respect to fire spread mode and vertical position within the flame, all of the Da exceed 10^6 (rounded to the nearest order of magnitude) which does not change the conclusion that the reactions are near equilibrium or "frozen" (Jenkins et al., 1993). Hence, we can conclude from this analysis that our emissions sampling is representative of the entire plume since the timescale required for the relevant chemical reactions to occur is very short relative to the flow timescale.

4.2 Equivalence of emissions factor reporting

In this section, we discuss a comparison between the two methods for reporting emission factors which are both based on a carbon mass balance approach (see section 2.4.1). As such, we switch interchangeably between reporting on a per unit element burnt basis (i.e. either fuel carbon or nitrogen) or a per unit dry fuel consumed basis. For our purposes, we define 'burnt' as fuel that has been thermally altered as a result of exposure to fire and either emitted to the atmosphere or left in the post-fire residue. We define 'consumed' as that component of the fuel that is emitted to the atmosphere as a result of exposure to fire. The relevant equation number or associated units are provided to make it clear which emissions factor reporting method we are using.

Comparison of the emissions factors reported per unit element burnt (Fig. 6) with those reported per unit of dry fuel consumed (Table 2) led to the apparently anomalous conclusion that CO_2 emission factors are greater for flanking and backing fires; a result which directly

contradicts those reported in Fig. 6. To properly resolve this apparent inconsistency, it is
5 important to realise that emissions factors calculated using either equation (2) or (5) are
only estimates and there are several sources of error. A source of error common to both
equations (2) or (5) arises because it is not possible to measure all the carbon compounds
present in the smoke plume.

If carbon-based emissions factors were to be calculated using only CO_2 , CO and CH_4
10 (which is a common approach), the total amount of carbon emitted would be underestimated
by 1–2% due to omitting NMHC and by a further 1–2% for neglecting PC (Yokelson et al.,
1999). The implication of not measuring all carbon emitted in the plume is that the emissions
factor would be over-estimated. Further sources of error include estimating the carbon frac-
15 tion deposited in ash (equation (2)) and estimating the fuel carbon content before burning
takes place (equation (5)). In atmospheric chemistry studies it is common to assume a fuel
carbon content of 50% (Paton-Walsh et al., 2014; Yokelson et al., 1999) whilst Hurst et al.
(1996) assumed that 6% of fuel carbon was deposited in ash. In this study, both the fuel
carbon fraction before burning and the fraction of carbon deposited in ash were measured,
meaning that these sources of error have been eliminated from the analysis.

20 A further source of error which has received limited discussion in the literature relates to
the equivalence of the methods described in equations (2) or (5). In particular, the calcula-
tion of total emissions from a fire should not depend on which metric is used to calculate
emissions factors. The method described in equation (2) is commonly used in inventory
reporting and is a well-established methodology. In contrast, applying equation (5) to esti-
25 mate total emissions would involve multiplying the area burnt, fuel load, combustion factor
and emissions factor and would not report the same result as equation (2). The reason for
this discrepancy is that the method described in equation (5) does not explicitly consider
the fraction of total fuel carbon emitted to the atmosphere. Instead, this method implicitly
assumes that all fuel carbon is emitted to the atmosphere.

Making the assumption that all fuel carbon is emitted to the atmosphere might be ac-
ceptable in the headfire of a high intensity wildfire; however, in the current work a signifi-
cant fraction of fuel carbon (12–30%) is contained in the post-fire residue and furthermore

5 displays a trend with respect to fire spread mode. As a result, in burning conditions representative of prescribed burning it is not acceptable to assume that all fuel carbon is emitted to the atmosphere and instead this fraction should be estimated, as recommended by Andreae and Merlet (2001) and as done in the current work. Multiplication of equation (5) by $\sum C_{emit}/C_{fuel}$ would enable the per unit dry fuel consumed method of reporting emissions
10 factors to report the same total emissions as the per unit element burnt method. Performing this correction leads to the correct trend in CO₂ emission factors with respect to fire spread mode, with heading fires (1407 g kg⁻¹) emitting more CO₂ than flanking (1200 g kg⁻¹) or backing fires (1284 g kg⁻¹).

4.3 Comparison with field derived measurements

15 This emissions study was performed in a combustion wind tunnel facility with the relationship of the results obtained with those acquired in the field constituting a very important validation exercise. Recently Volkova et al. (2014) explored the relationship of fuel reduction burning on the carbon and greenhouse gas emissions from subsequent wildfire in temperate forest in Victoria, Australia. Measurements of CH₄ and N₂O emission factors over
20 a very wide MCE range (0.7-1) were made during fuel reduction burning. The laboratory-derived CH₄ and N₂O emissions factors are in very good agreement with those measured by Volkova et al. who measured CH₄ emission factors (reported per unit element burnt) between 0.5-1.5% and N₂O emission factors between 0.4-1% over the MCE range relevant to the laboratory measurements (0.82-0.93).

25 Another valuable source of data for comparison is the dataset of Paton-Walsh et al. (2014) who recently measured trace gas emissions factors with an FTIR system during prescribed fires in temperate forests in New South Wales, Australia. Our CO₂ emissions factors (reported per unit of dry fuel consumed) are slightly smaller for heading fires (~1.5%) and are larger for flanking (~5%) and backing fires (~6%) compared to Paton-Walsh et al. Keeping in mind that emissions sampling from an active fire front will involve contributions from different fire spread modes (especially heading and flanking) makes the overall CO₂ emissions profile from our measurements consistent with those reported by Paton-Walsh et al.

Our CO emissions factors (reported per unit of dry fuel consumed) are significantly higher for heading fires (~45%) due to significant smouldering after the progression of the flame front (see Fig. 8), but are lower for flanking (~17%) and backing fires (~19%). Our CH₄ emission factors (reported per unit of dry fuel consumed) are higher for heading (20%) and flanking (~23%) fires but are slightly lower for backing (~6%) fires. Increases in our CH₄ and CO emissions factors are consistent with sampling at a lower MCE in the combustion wind tunnel compared to the results of Paton-Walsh et al. Our MCE range was 0.82–0.93, whereas the recommended emissions factors reported by Paton-Walsh et al. are based on an MCE average of 0.90. In contrast our N₂O emissions factors (reported per unit of dry fuel consumed) are lower for heading (~41%), flanking (22%) and backing (~57%) compared to Paton-Walsh et al.

The only other published estimates of greenhouse gas emissions from temperate forest fires in Australia are those of Hurst et al. (1996) who measured CO₂, CO and CH₄ emission factors for two wildfires in the Sydney region in February 1991, another wildfire in January 1994 and also a prescribed fire in March 1994. Averaged over four fires, they measured emission factors (reported per unit element burnt) of 85% for CO₂, 9.1% for CO and 0.54% for CH₄. They did not measure fuel consumption; however, the production of ash was assumed to be 6% of total fuel carbon. As seen from Fig. 6, the post-burn residue fraction in our study was much larger than that reported by Hurst et al. (1996), which places an upper limit on how much fuel carbon can be released as CO₂. As a result, CO₂ emissions factors measured by Hurst et al. are substantially higher than those we measured; however our range of CO emissions factors was similar to those reported by Hurst et al. CH₄ emission factors for heading fires were very similar in magnitude to those reported by Hurst et al. with CH₄ emissions factors from flanking and backing fires being slightly less than those from heading fires. Therefore, based on comparison of our results with three field sampling studies suggests that the design of the CSIRO Pyrotron has successfully captured the combustion and emissions dynamics that typically occur under prescribed burning conditions.

5 4.4 A comment on N₂O emissions production

As highlighted by van Leeuwen et al. (2013), exploring the temporal variability of emissions factors from biomass burning is an important consideration but is rarely undertaken. Despite reports in the literature of N₂O emissions factors being dominant in flaming combustion (Lobert et al., 1990; Urbanski, 2013), there is strong evidence from Fig. 8 of contributions to N₂O emissions from both flaming and smouldering combustion. This fact is evident from Fig. 8b by looking at the limited temporal variability in the N₂O emissions factor (with respect to time) compared to other emissions species. Clearly further measurements and modelling work is required to develop a mechanistic understanding of N₂O emissions production from fire.

15 4.5 Implications for carbon accounting and sequestration

The results from this study have implications for both the mitigation of greenhouse gas emissions from fire and also carbon accounting methods which we discuss with reference to prescribed burning in Victoria. The Royal Commission into the 2009 bushfires in Victoria recommended that 5% of Victoria's public land (approximately 390 000 hectares) should be burnt by prescribed fires each year to reduce the risk of bushfires (Teague et al., 2010). Using state-based and country specific data from Australia's National Inventory System (Commonwealth of Australia, 2014) it is estimated that 5630 Gigagrams (Gg) of CO₂ equivalent (CO₂-e) emissions would be emitted from the burning of 390 000 hectares. Using the emission and combustion factors derived from our experimental study (as an estimate of prescribed burning emission and combustion factors) and keeping all other inputs fixed yields estimates of: 5640 Gg of CO₂-e emissions if all the area is burnt by heading fire, 4200 Gg CO₂-e if burnt by flanking fire and 4990 Gg CO₂-e if burnt as a backing fire. Whilst it would not be possible to apply a single fire spread mode to a forested landscape in a prescribed fire situation, ignition patterns are practised in Victoria which enable a single fire spread mode to predominate (Tolhurst and Cheney, 1999), such as the three investigated in this study.

This calculation suggests that the preferential application of flanking fires over heading fires during prescribed burning operations would save approximately 1280 Gg of CO₂ emissions with 420 Gg being saved with backing fires. In addition, the application of flanking fires would leave an extra 265 Gg of carbon as a post-fire combustion residue (compared to heading fires) and backing fires would leave an extra 250 Gg; preventing further carbon emissions to the atmosphere. A further benefit to the application of non-heading fires during prescribed burning would be a reduction in CO emissions, which are implicated in respiratory health effects, with flanking fires emitting 330 Gg less CO (compared to heading fires) and backing fires emitting 290 Gg less.

In addition, the results have implications for carbon accounting methods considering that the Australia's National Inventory System does not currently discriminate between types of fire other than whether they are prescribed or wildfires. Given that, compared with heading fires, CO₂-e emissions are about 26% lower for flanking fires and 11% lower for backing fires, there is potentially scope for more accurate greenhouse inventory reporting by taking into account the mode of fire spread.

5 Conclusions

This study has explored the hypothesis (which was formulated and tested statistically) that fire spread mode and phase of combustion could lead to differences in emission factors of greenhouse gases from laboratory-scale fires conducted in a wind tunnel facility. We found that both fire spread mode and combustion phase had statistically significant impacts on emissions of greenhouse gases. Furthermore, the temporal progression of emission factors were markedly different for the three different fire spread modes.

In particular, we found that flanking and backing fires emitted less CO₂ and CO than heading fires and had more carbon remaining in combustion residues on a per unit carbon basis. These results have direct relevance to the management of forested landscapes that are affected by fire. Given the lower magnitude of greenhouse emissions species from flanking and backing fires this (potentially) opens up an opportunity to reduce carbon emis-

sions from fire by the strategic use of these fire spread modes over heading fires. Future
10 research activities could involve investigating greenhouse gas emissions for different fire
spread modes but with more strata in the fuel bed which would better represent the way in
which forest fuels burn in the field. In addition, the measurement of particulate emissions
factors continues to be a significant avenue for future research.

Author contributions

15 All authors were involved in the experimental design. NCS, ALS and SHR performed the
experiments with guidance from PJP. NCS performed the data analysis with input from ALS
and CPM. NCS prepared the manuscript with contributions from all co-authors.

Acknowledgements

20 The authors thank Mr Nigel England and Dr Matthew Plucinski for their assistance during
the experimental fires. This work was undertaken in the former Greenhouse Gas Abatement
and Carbon Storage in Land Use Systems Theme of the Sustainable Agriculture Flagship.
The authors wish to thank Dr Michael Battaglia and Dr Sandra Eady for their support of this
project and their guidance.

References

- 25 Akagi, S. K., Yokelson, R. J., Wiedinmyer, C., Alvarado, M. J., Reid, J. S., Karl, T., Crouse, J. D., and
Wennberg, P. O.: Emission factors for open and domestic biomass burning for use in atmospheric
models, *Atmospheric Chemistry and Physics*, 11, 4039–4072, doi:10.5194/acp-11-4039-2011,
2011.
- Andreae, M. O. and Merlet, P.: Emission of trace gases and aerosols from biomass burning, *Global
Biogeochemical Cycles*, 15, 955–966, doi:10.1029/2000gb001382, 2001.

- Baer, D. S., Paul, J. B., Gupta, J. B., and O'Keefe, A.: Sensitive absorption measurements in the near-infrared region using off-axis integrated-cavity-output spectroscopy, *Applied Physics B-Lasers and Optics*, 75, 261–265, doi:10.1007/s00340-002-0971-z, 2002.
- 5 Bowman, D. M. J. S., Balch, J. K., Artaxo, P., Bond, W. J., Carlson, J. M., Cochrane, M. A., D'Antonio, C. M., DeFries, R. S., Doyle, J. C., Harrison, S. P., Johnston, F. H., Keeley, J. E., Krawchuk, M. A., Kull, C. A., Marston, J. B., Moritz, M. A., Prentice, I. C., Roos, C. I., Scott, A. C., Swetnam, T. W., van der Werf, G. R., and Pyne, S. J.: Fire in the Earth System, *Science*, 324, 481–484, doi:10.1126/science.1163886, 2009.
- 10 Byram, G. M.: Combustion of forest fuels, in: *Forest Fire Control and Use*, edited by Davis, K., pp. 61–89, McGraw-Hill, New York, 1959.
- Cai, W., Cowan, T., and Raupach, M.: Positive Indian Ocean Dipole events precondition southeast Australia bushfires, *Geophysical Research Letters*, 36, L19710, doi:10.1029/2009gl039902, 2009.
- Chatto, K. and Tolhurst, K.: The development and testing of the Wiltronics T-H fine fuel moisture meter, Research Report No. 46, Fire Management Branch, Department of Natural Resources and Environment, Melbourne, Victoria, 1997.
- 15 Cheney, N. P.: Fire behaviour, in: *Fire and the Australian biota*, edited by Gill, A. M., Groves, R. H., and Noble, I. R., pp. 151–176, The Australian Academy of Science, Canberra, 1981.
- Commonwealth of Australia: Australian National Greenhouse Accounts, National Inventory Report 2012, Volume 2, Department of Environment, Canberra, 2014.
- 20 Crutzen, P. J., Heidt, L. E., Krasnec, J. P., Pollock, W. H., and Seiler, W.: Biomass burning as a source of atmospheric gases CO, H₂, N₂O, NO, CH₃CL and COS, *Nature*, 282, 253–256, doi:10.1038/282253a0, 1979.
- Cruz, M., Sullivan, A., Gould, J., Sims, N., Bannister, A., Hollis, J., and Hurley, R.: Anatomy of a catastrophic wildfire: the Black Saturday Kilmore East fire in Victoria, Australia, *Forest Ecology and Management*, 284, 269–285, doi:10.1016/j.foreco.2012.02.035, 2012.
- Department of Agriculture: Australian Coastal Outline and Landmass with State Boundaries, http://data.daff.gov.au/anrdl/metadata_files/pa_nsaasr9nnd_02211a04.xml, (last access: 4 September 2014), 2014.
- 30 Houghton, R. A., Hall, F., and Goetz, S. J.: Importance of biomass in the global carbon cycle, *Journal of Geophysical Research-Biogeosciences*, 114, G00E03, doi:10.1029/2009jg000935, 2009.
- Hurst, D. F., Griffith, D. W. T., Carras, J. N., Williams, D. J., and Fraser, P. J.: Measurements of trace gases emitted by Australian savanna fires during the 1990 dry season, *Journal of Atmospheric Chemistry*, 18, 33–56, doi:10.1007/bf00694373, 1994a.

Hurst, D. F., Griffith, D. W. T., and Cook, G. D.: Trace gas emissions from biomass burning in tropical Australian savannas, *Journal of Geophysical Research-Atmospheres*, 99, 16 441–16 456, doi:10.1029/94jd00670, 1994b.

5 Hurst, D. F., Griffith, D. W. T., and Cook, G. D.: Trace-gas emissions from biomass burning in Australia, in: *Biomass burning and global change*, edited by Levine, J., vol. 2, pp. 787–792, The MIT Press, Cambridge, Massachusetts, 1996.

Jenkins, B. M., Kennedy, I. M., Turn, S. Q., Williams, R. B., Hall, S. G., Teague, S. V., Chang, D. P. Y., and Raabe, O. G.: Wind-tunnel modeling of atmospheric emissions from agricultural burning - influence of operating configuration on flame structure and particle-emission factor for a spreading-type fire, *Environmental Science & Technology*, 27, 1763–1775, doi:10.1021/es00046a002, 1993.

10 Keene, W. C., Lobert, J. M., Crutzen, P. J., Maben, J. R., Scharffe, D. H., Landmann, T., Hély, C., and Brain, C.: Emissions of major gaseous and particulate species during experimental burns of southern African biomass, *Journal of Geophysical Research-Atmospheres*, 111(D4), doi:10.1029/2005jd006319, 2006.

15 Law, C. K.: *Combustion Physics*, Cambridge University Press, New York, 2006.

Le Canut, P., Andreae, M. O., Harris, G. W., Wienhold, F. G., and Zenker, T.: Airborne studies of emissions from savanna fires in southern Africa.1. Aerosol emissions measured with a laser optical particle counter, *Journal of Geophysical Research-Atmospheres*, 101, 23 615–23 630, doi:10.1029/95jd02610, 1996.

20 Lee, T., Sullivan, A. P., Mack, L., Jimenez, J. L., Kreidenweis, S. M., Onasch, T. B., Worsnop, D. R., Malm, W., Wold, C. E., Hao, W. M., and Collett, Jeffrey L., J.: Chemical smoke marker emissions during flaming and smoldering phases of laboratory open burning of wildland fuels, *Aerosol Science and Technology*, 44, I–V, doi:10.1080/02786826.2010.499884, 2010.

25 Levine, J. and Cofer III, W.: Boreal forest fire emissions and the chemistry of the atmosphere, in: *Fire, Climate Change, and Carbon Cycling in the Boreal Forest*, edited by Kasischke, E. S. and Stocks, B. J., pp. 31–48, Springer-Verlag, New York, 2000.

Lobert, J. M., Scharffe, D. H., Hao, W. M., and Crutzen, P. J.: Importance of biomass burning in the atmospheric budgets of nitrogen-containing gases, *Nature*, 346, 552–554, doi:10.1038/346552a0, 1990.

30 Mack, M. C., Bret-Harte, M. S., Hollingsworth, T. N., Jandt, R. R., Schuur, E. A. G., Shaver, G. R., and Verbyla, D. L.: Carbon loss from an unprecedented Arctic tundra wildfire, *Nature*, 475, 489–492, doi:10.1038/nature10283, 2011.

- Matthews, S.: Effect of drying temperature on fuel moisture content measurements, *International Journal of Wildland Fire*, 19, 800–802, doi:10.1071/WF08188, 2010.
- McArthur, A.: Control burning in eucalypt forests, *Forestry and Timber Bureau No. 80, Commonwealth of Australia, Canberra*, 1962.
- 5 McArthur, A.: Fire Behaviour in Eucalypt Forests, *Forest and Timber Bureau Leaflet No. 107, Commonwealth of Australia, Canberra*, 1967.
- McMeeking, G. R., Kreidenweis, S. M., Baker, S., Carrico, C. M., Chow, J. C., Collett, Jr., J. L., Hao, W. M., Holden, A. S., Kirchstetter, T. W., Malm, W. C., Moosmüller, H., Sullivan, A. P., and Wold, C. E.: Emissions of trace gases and aerosols during the open combustion of biomass in the laboratory, *Journal of Geophysical Research-Atmospheres*, 114, doi:10.1029/2009JD011836, 10 2009.
- Meyer, C. P. and Cook, G. D.: Biomass combustion and emission processes in the Northern Australian Savannas, in: *Carbon Accounting and Savanna Fire Management*, CSIRO Publishing, Collingwood, Australia, 2015, In press.
- 15 Meyer, C. P., Cook, G. D., Reisen, F., Smith, T. E. L., Tattaris, M., Russell-Smith, J., Maier, S. W., Yates, C. P., and Wooster, M. J.: Direct measurements of the seasonality of emission factors from savanna fires in northern Australia, *Journal of Geophysical Research-Atmospheres*, 117, doi:10.1029/2012jd017671, 2012.
- Monks, P. S., Granier, C., Fuzzi, S., Stohl, A., Williams, M. L., Akimoto, H., Amann, M., Baklanov, A., Baltensperger, U., Bey, I., Blake, N., Blake, R. S., Carslaw, K., Cooper, O. R., Dentener, F., Fowler, D., Fragkou, E., Frost, G. J., Generoso, S., Ginoux, P., Grewe, V., Guenther, A., Hansson, H. C., Henne, S., Hjorth, J., Hofzumahaus, A., Huntrieser, H., Isaksen, I. S. A., Jenkin, M. E., Kaiser, J., Kanakidou, M., Klimont, Z., Kulmala, M., Laj, P., Lawrence, M. G., Lee, J. D., Liousse, C., Maione, M., McFiggans, G., Metzger, A., Mieville, A., Moussiopoulos, N., Orlando, J. J., O'Dowd, C. D., 20 Palmer, P. I., Parrish, D. D., Petzold, A., Platt, U., Pöschl, U., Prévôt, A. S. H., Reeves, C. E., Reimann, S., Rudich, Y., Sellegri, K., Steinbrecher, R., Simpson, D., ten Brink, H., Theloke, J., van der Werf, G. R., Vautard, R., Vestreng, V., Vlachokostas, C., and von Glasow, R.: Atmospheric composition change - global and regional air quality, *Atmospheric Environment*, 43, 5268–5350, doi:10.1016/j.atmosenv.2009.08.021, 2009.
- 25 30 Mulvaney, J.: The Inherent Variability of Fires in Naturally Heterogeneous Fuel Beds under Controlled Conditions, Honours thesis, Fenner School of Environment and Society, Australian National University, Canberra, 2012.

- O'Keefe, A. and Deacon, D. A. G.: Cavity ring-down optical spectrometer for absorption-measurements using pulsed laser sources, *Review of Scientific Instruments*, 59, 2544–2551, doi:10.1063/1.1139895, 1988.
- Paton-Walsh, C., Smith, T. E. L., Young, E. L., Griffith, D. W. T., and Guérette, É. A.: New emission factors for Australian vegetation fires measured using open-path Fourier transform infrared spectroscopy - Part 1: methods and Australian temperate forest fires, *Atmospheric Chemistry and Physics Discussion*, 14, 4327–4381, doi:10.5194/acpd-14-4327-2014, 2014.
- Radke, L., Hegg, D., Lyons, J., Brock, C., and Hobbs, P.: Airborne measurements on smokes from biomass burning, in: *Aerosols and climate*, edited by Hobbs, P. and Patrick McCormick, M., pp. 411–422, A. Deepak Publishing, Hampton, Virginia, 1988.
- Ranzi, E., Cuoci, A., Faravelli, T., Frassoldati, A., Migliavacca, G., Pierucci, S., and Sommariva, S.: Chemical Kinetics of Biomass Pyrolysis, *Energy & Fuels*, 22, 4292–4300, doi:10.1021/ef800551t, 2008.
- Reid, J. S., Koppmann, R., Eck, T. F., and Eleuterio, D. P.: A review of biomass burning emissions part II: intensive physical properties of biomass burning particles, *Atmospheric Chemistry and Physics*, 5, 799–825, doi:10.5194/acp-5-799-2005, 2005.
- Running, S. W.: Is global warming causing more, larger wildfires?, *Science*, 313, 927–928, doi:10.1126/science.1130370, 2006.
- Seiler, W. and Crutzen, P. J.: Estimates of gross and net fluxes of carbon between the biosphere and the atmosphere from biomass burning, *Climatic Change*, 2, 207–247, doi:10.1007/bf00137988, 1980.
- Sullivan, A. L. and Ball, R.: Thermal decomposition and combustion chemistry of cellulosic biomass, *Atmospheric Environment*, 47, 133–141, doi:10.1016/j.atmosenv.2011.11.022, 2012.
- Sullivan, A. L. and Matthews, S.: Determining landscape fine fuel moisture content of the Kilmore East 'Black Saturday' wildfire using spatially-extended point-based models, *Environmental Modelling & Software*, 40, 98–108, doi:10.1016/j.envsoft.2012.08.008, 2013.
- Sullivan, A. L., McCaw, W., Cruz, M., Matthews, S., and Ellis, P.: Fuel, fire weather and fire behaviour in Australian ecosystems, in: *Flammable Australia: fire regimes, biodiversity and ecosystems in a changing world*, edited by Bradstock, R., Gill, A., and Williams, R., pp. 51–77, CSIRO publishing, Collingwood, Victoria, 2012.
- Sullivan, A. L., Knight, I. K., Hurley, R. J., and Webber, C.: A contractionless, low-turbulence wind tunnel for the study of free-burning fires, *Experimental Thermal and Fluid Science*, 44, 264–274, doi:10.1016/j.expthermflusci.2012.06.018, 2013.

- Teague, B., McLeod, R., and Pascoe, S.: 2009 Victorian Bushfires Royal Commission, Final report summary, State of Victoria, Melbourne, Victoria, 2010.
- Tolhurst, K. G. and Cheney, N. P.: Synopsis of the knowledge used in prescribed burning in Victoria, Department of Natural Resources and Environment, East Melbourne, Victoria, 1999.
- Urbanski, S. P.: Combustion efficiency and emission factors for wildfire-season fires in mixed conifer forests of the northern Rocky Mountains, US, *Atmospheric Chemistry and Physics*, 13, 7241–7262, doi:10.5194/acp-13-7241-2013, 2013.
- van der Werf, G. R., Randerson, J. T., Giglio, L., Collatz, G. J., Mu, M., Kasibhatla, P. S., Morton, D. C., DeFries, R. S., Jin, Y., and van Leeuwen, T. T.: Global fire emissions and the contribution of deforestation, savanna, forest, agricultural, and peat fires (1997-2009), *Atmospheric Chemistry and Physics*, 10, 11 707–11 735, doi:10.5194/acp-10-11707-2010, 2010.
- van Leeuwen, T. T. and van der Werf, G. R.: Spatial and temporal variability in the ratio of trace gases emitted from biomass burning, *Atmospheric Chemistry and Physics*, 11, 3611–3629, doi:10.5194/acp-11-3611-2011, 2011.
- van Leeuwen, T. T., Peters, W., Krol, M. C., and van der Werf, G. R.: Dynamic biomass burning emission factors and their impact on atmospheric CO mixing ratios, *Journal of Geophysical Research-Atmospheres*, 118, 6797–6815, doi:10.1002/jgrd.50478, 2013.
- Vicente, A., Alves, C., Monteiro, C., Nunes, T., Mirante, F., Evtugina, M., Cerqueira, M., and Pio, C.: Measurement of trace gases and organic compounds in the smoke plume from a wildfire in Penedono (central Portugal), *Atmospheric Environment*, 45, 5172–5182, doi:10.1016/j.atmosenv.2011.06.021, 2011.
- Volkova, L., Meyer, C. P. M., Murphy, S., Fairman, T., Reisen, F., and Weston, C.: Fuel reduction burning mitigates wildfire effects on forest carbon and greenhouse gas emission, *International Journal Of Wildland Fire*, 23, 771–780, doi:10.1071/WF14009, 2014.
- Weinhold, B.: Fields and forests in flames: Vegetation smoke and human health, *Environmental Health Perspectives*, 119, A386–A393, doi:10.1289/ehp.119-a386, 2011.
- Wotton, B. M., Gould, J. S., McCaw, W. L., Cheney, N. P., and Taylor, S. W.: Flame temperature and residence time of fires in dry eucalypt forest, *International Journal Of Wildland Fire*, 21, 270–281, doi:10.1071/WF10127, 2012.
- Yokelson, R. J., Goode, J. G., Ward, D. E., Susott, R. A., Babbitt, R. E., Wade, D. D., Bertschi, I., Griffith, D. W. T., and Hao, W. M.: Emissions of formaldehyde, acetic acid, methanol, and other trace gases from biomass fires in North Carolina measured by airborne Fourier trans-

form infrared spectroscopy, *Journal of Geophysical Research-Atmospheres*, 104, 30 109–30 125, doi:10.1029/1999jd900817, 1999.

745

Yokelson, R. J., Burling, I. R., Gilman, J. B., Warneke, C., Stockwell, C. E., de Gouw, J., Akagi, S. K., Urbanski, S. P., Veres, P., Roberts, J. M., Kuster, W. C., Reardon, J., Griffith, D. W. T., Johnson, T. J., Hosseini, S., Miller, J. W., Cocker III, D. R., Jung, H., and Weise, D. R.: Coupling field and laboratory measurements to estimate the emission factors of identified and unidentified trace gases for prescribed fires, *Atmospheric Chemistry and Physics*, 13, 89–116, doi:10.5194/acp-13-89-2013, 2013.

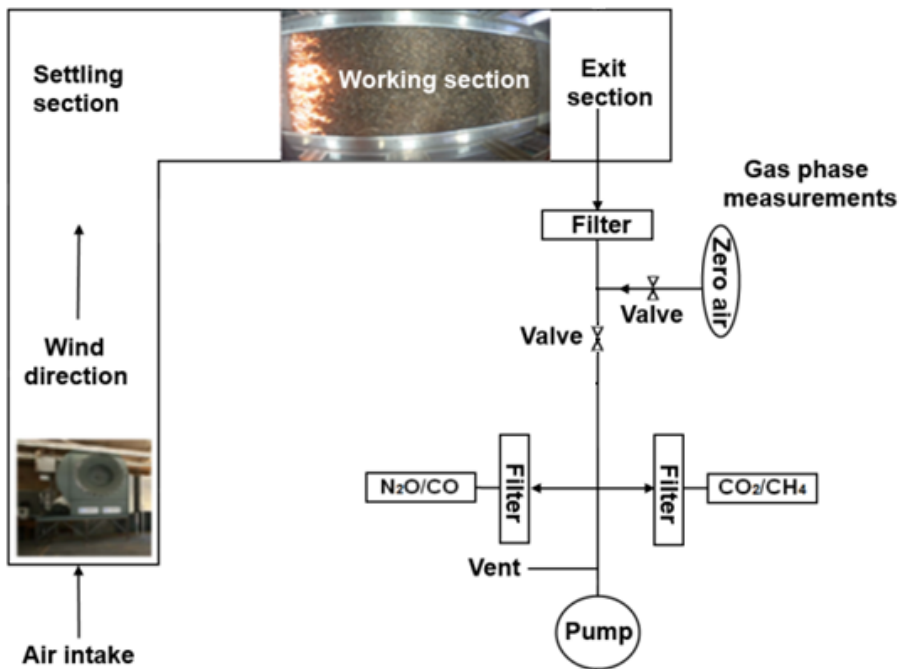


Figure 1. A schematic (not to scale) of the experimental configuration used in the CSIRO Pyrotron for experimental fires.

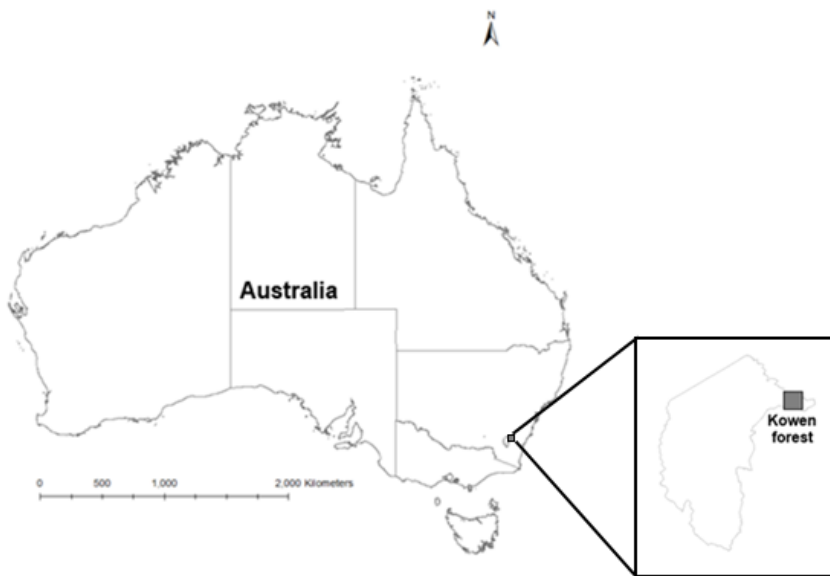


Figure 2. Location of the dry sclerophyll eucalypt forest for collection of litter ($35^{\circ} 19' 30.07''$ S, $149^{\circ} 15' 25.64''$ E). Shapefile of Australia sourced from Department of Agriculture (2014).

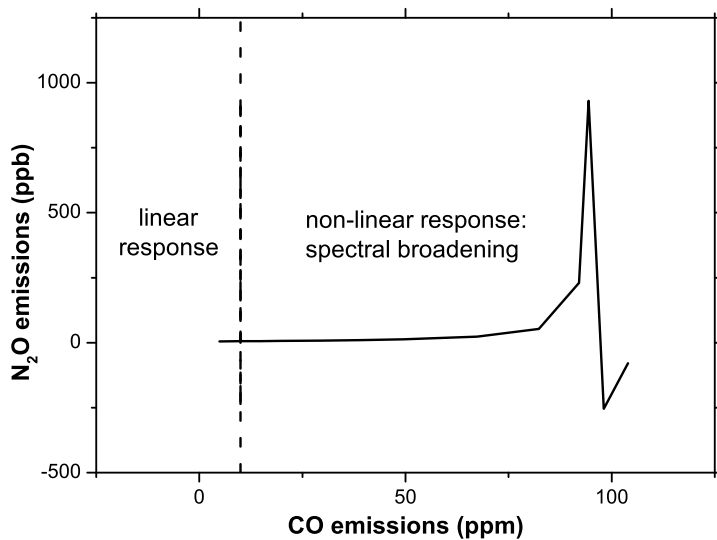


Figure 3. A graph of the interaction between N₂O and CO emissions measurements during routine calibrations which necessitated the use of a dilution system.

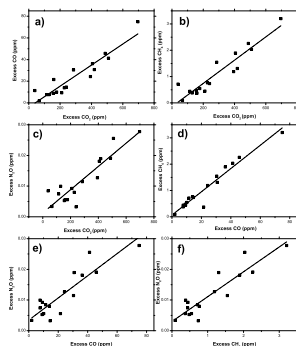


Figure 4. Linear fits of excess mixing ratios for all 18 experimental fires (not corrected for the overall dilution ratio) using either CO_2 , CO or CH_4 as a reference gas. a): CO plotted against CO_2 ($R^2=0.872$, $\text{CO}=-3.99+0.097\text{CO}_2$). b): CH_4 plotted against CO_2 ($R^2=0.871$, $\text{CH}_4=-0.14+0.0044\text{CO}_2$). c): N_2O plotted against CO_2 ($R^2=0.811$, $\text{N}_2\text{O}=0.0012+3.79\times 10^{-5}\text{CO}_2$). d): CH_4 plotted against CO ($R^2=0.942$, $\text{CH}_4=-0.066+0.044\text{CO}$). e): N_2O plotted against CO ($R^2=0.788$, $\text{N}_2\text{O}=0.0035+3.61\times 10^{-4}\text{CO}$). f): N_2O plotted against CH_4 ($R^2=0.822$, $\text{N}_2\text{O}=0.0030+0.0081\text{CH}_4$).

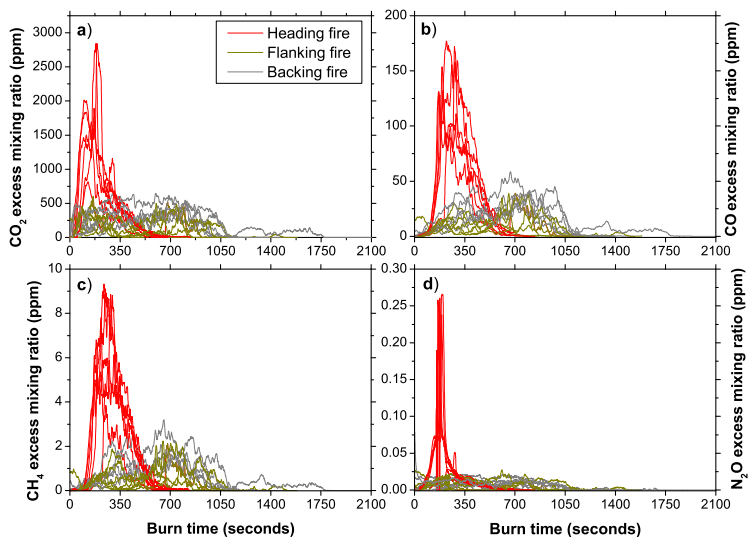


Figure 5. Time series of excess mixing ratios for different emissions species and three different fire spread modes a): CO₂. b): CO. c): CH₄. d): N₂O. Note that each line of a particular colour represents one experimental replicate.

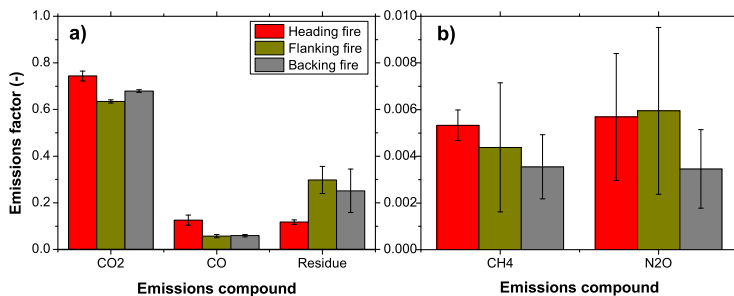


Figure 6. Carbon and nitrogen based emissions factors (per unit of carbon or nitrogen burnt) from the experimental burns. a): CO₂, CO and residue carbon emission factors. b): CH₄ and N₂O emission factors.

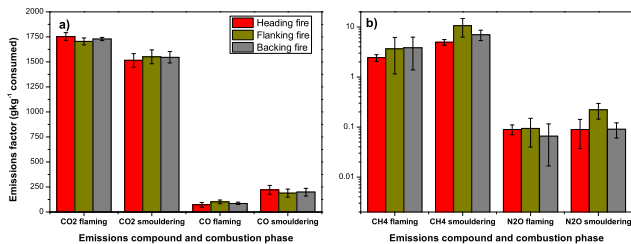


Figure 7. Carbon and nitrogen based emissions factors (per unit of dry matter burnt) for different combustion phases within the experimental burns. a): CO₂ and CO emission factors for flaming and smouldering combustion. b): CH₄ and N₂O emission factors for flaming and smouldering combustion.

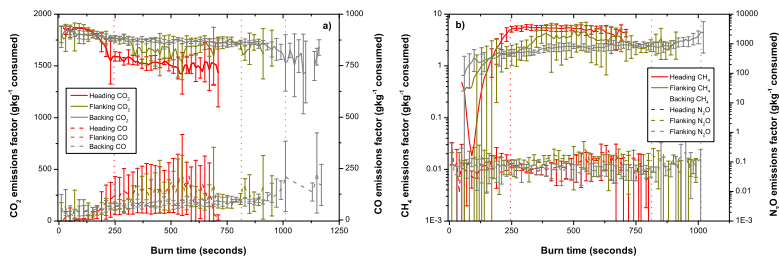


Figure 8. Time resolved emissions factors for the trace gas emissions species measured during the experimental burns. a): time resolved CO_2 and CO emissions factors. b): time resolved CH_4 and N_2O emissions factors. Coloured vertical and dotted bars represent the median end time for predominantly flaming combustion for each fire spread mode.

Table 1. Summary data from the fire experiments. Values are reported as the mean with the range reported as: (minimum value–maximum value). Byram fireline intensity is the product of the lower heating value of the fuel (kJ kg^{-1}), fuel consumed (kg m^{-2}) and the forward rate of spread (m s^{-1}) Byram (1959).

| Fire spread mode | Fuel moisture content (%) | Fire duration (s) | Flaming combustion duration (s) | Smouldering combustion duration (s) | Rate of spread (m h^{-1}) | Combustion factor (-) | Residue carbon content (%) | Byram fireline intensity (kW m^{-1}) |
|------------------|---------------------------|-------------------|---------------------------------|-------------------------------------|--------------------------------------|-----------------------|----------------------------|---|
| Heading | 5.6 (5.0–6.8) | 715 (580–840) | 256 (224–290) | 459 (356–582) | 123 (103–150) | 81.8 (77.7–84.4) | 33.3 (29.4–66.2) | 553 (462–693) |
| Flanking | 5.6 (5.1–6.2) | 1085 (900–1530) | 907 (763–1099) | 178 (93–431) | 6.6 (4.9–8.2) | 71.6 (61.3–81.7) | 54.0 (39.2–67.7) | 26 (17–32) |
| Backing | 5.4 (4.6–6.5) | 1413 (1160–2230) | 1196 (867–1988) | 218 (72–533) | 6.1 (4.2–7.5) | 82.2 (77.3–86.4) | 72.8 (34.8–78.9) | 27 (20–32) |

Table 2. Emissions factors (\pm one standard deviation) for emissions species reported on a per unit of dry fuel burnt basis.

| Data source | CO ₂ (g kg ⁻¹) | CO (g kg ⁻¹) | CH ₄ (g kg ⁻¹) | N ₂ O (g kg ⁻¹) |
|-----------------------------|---------------------------------------|--------------------------|---------------------------------------|--|
| Heading fires (this study) | 1594 \pm 46 | 172 \pm 30 | 4.2 \pm 0.5 | 0.089 \pm 0.043 |
| Flanking fires (this study) | 1709 \pm 18 | 98 \pm 11 | 4.3 \pm 2.7 | 0.117 \pm 0.071 |
| Backing fires (this study) | 1716 \pm 14 | 95 \pm 9 | 3.3 \pm 1.3 | 0.064 \pm 0.031 |
| Andreae and Merlet (2001) | 1569 \pm 131 | 107 \pm 37 | 4.7 \pm 1.9 | 0.26 \pm 0.07 |
| Akagi et al. (2011) | 1637 \pm 71 | 89 \pm 32 | 3.9 \pm 2.4 | 0.16 \pm 0.21 |
| Paton-Walsh et al. (2014) | 1620 \pm 30 | 118 \pm 16 | 3.5 \pm 1.1 | 0.15 \pm 0.09 |

Table 3. Calculation of the reaction Damköhler number (Da) for several axial positions and flame heights within the flame.

| Fire spread mode | $T_{\text{flame tip}}$ (K) | $T_{\text{flame base}}$ (K) | τ_F (s) | τ_C flame tip | τ_C flame base | $Da_{\text{flame tip}}$ | $Da_{\text{flame base}}$ |
|------------------|----------------------------|-----------------------------|--------------|----------------------|----------------------|-------------------------|--------------------------|
| Heading | 540 | 1170 | 5.6 | 8.0×10^{-7} | 2.2×10^{-8} | 7.0×10^6 | 2.6×10^8 |
| Heading | 540 | 1170 | 2.4 | 8.0×10^{-7} | 2.2×10^{-8} | 3.0×10^6 | 1.1×10^8 |
| Flanking | 540 | 1050 | 5.6 | 8.0×10^{-7} | 3.1×10^{-8} | 7.0×10^6 | 1.8×10^8 |
| Flanking | 540 | 1050 | 2.4 | 8.0×10^{-7} | 3.1×10^{-8} | 3.0×10^6 | 7.7×10^7 |
| Backing | 540 | 1220 | 5.6 | 8.0×10^{-7} | 1.9×10^{-8} | 7.0×10^6 | 2.9×10^8 |
| Backing | 540 | 1220 | 2.4 | 8.0×10^{-7} | 1.9×10^{-8} | 3.0×10^6 | 1.3×10^8 |